RESEARCH PAPER

PCCP
www.rsc.org/pccp

Adsorption and surface mobility of cinchonidine on Pt(111) studied by STM†

Matthias von Arx,*[ab] Markus Wahl,[b] Thomas A. Jung[bc] and Alfons Baiker[a]

[a] *Departement für Chemie und Angewandte Biowissenschaften, ETH Hönggerberg CH-8093 Zürich, Switzerland. E-mail: vonarx@chem.ethz.ch; Fax: +41 1 632 11 63; Tel: +41 1 633 45 52*
[b] *Institut für Physik der Universität Basel, Klingelbergstrasse 82, CH-4056 Basel*
[c] *Labor für Mikro- und Nanotechnologie, PSI, CH-5232 Villigen, Switzerland*

Received 5th May 2004, Accepted 15th October 2004
First published as an Advance Article on the web 26th October 2004

The adsorption of cinchonidine (CD) on Pt(111) has been investigated by means of STM in the presence and absence of hydrogen. The time-resolved studies revealed that the mobility of adsorbed CD molecules depends on the hydrogen pressure. At low hydrogen pressure the CD molecules are rather immobile, whereas considerable mobility is observed at higher hydrogen pressure. Based on the different adsorption geometries and the surface mobility three different species could be distinguished and their dynamic behaviour was investigated on a single molecule level.

Introduction

The investigation of complex organic molecules on metal surfaces by scanning probe microscopies (SPM) has become a topic of great interest in recent years. Most of the research has been centered on the study of molecular self assembly on rather unreactive metal surfaces (For a few selected examples, see refs. 1–3). Much less is known about the behaviour and the surface chemistry of molecules on more reactive surfaces, as used in catalysis.

Particularly challenging is the study of the behaviour of chiral molecules adsorbed on catalytically active metal surfaces due to its relevance to asymmetric heterogeneous catalysis. Today three catalytic systems based on chiral modification of active metal surfaces are known, which afford an enantiomeric excess over 90% for the hydrogenation of certain substrates. These are the Ni–tartaric acid, Pt–cinchona and Pd–cinchona systems.[4–6] The Ni–tartaric acid system has been investigated by means of STM by Raval and coworkers.[7,8] The platinum–cinchona system has been adressed recently with a combined STM-photoelectron spectroscopy approach by the group of Lambert.[9,10] However, this work focused mainly on the oligomerization of the reactant methyl pyruvate (MP) and the adsorption of the simplified modifier (*S*)-1-(1-naphthyl)ethylamine, which is not an actual chiral modifier but a precursor to a chiral modifier for enantioselective hydrogenation on Pt.[11] For cinchonidine (CD), the most powerful modifier, only STM studies on Cu(111) exist so far.[12,13] However, copper is not active for this type of reaction and therefore the observed assembly of CD is unlikely to be relevant for the catalytic system.

The aim of the present study was to gain direct insight in the molecular processes which occur during adsorption of cinchonidine on Pt(111). We could identify two different adsorption modes of CD, observe its conformational flexibility and follow the change in adsorption geometry upon addition of hydrogen. Our findings are discussed in the light of catalytic, theoretical and spectroscopic data available for this system. The time-resolved STM investigations uncovered details of the dynamic surface processes, which would be hardly accessible by other surface analytical techniques.

Experimental

All experiments were performed in a multichamber ultrahigh vacuum system, providing different preparation and characterization methods. The Pt(111) single crystal was cleaned by repeated Ar ion etching (800 eV, 4×10^{-7} mbar) and subsequent annealing to 1000 K *via* electron impact. Annealing, at times, in the presence of a standing oxygen pressure of 5×10^{-8} mbar led to an atomically clean Pt surface. The cinchonidine molecules were deposited by sublimation from a resistively heated tantalum crucible at a maximum temperature of 200 °C. The pressure during deposition was 7×10^{-10} mbar. A custom-built quartz microbalance was used to measure the deposition rate and the coverage. The mild deposition parameters used (200 °C crucible temperature, 25 °C sample temperature)[14] should guarantee that CD is deposited and adsorbed on Pt(111) as an intact entity. Intact adsorption is also supported by the lack of any evidence of CD fragmentation found at room temperature by IR-spectroscopic investigations of CD adsorption on Pt, as reported earlier.[15,16]

The hydrogen pressure in the range of 1×10^{-10} mbar to 5×10^{-6} mbar was controlled by a leak valve. All samples were measured by a home-built STM at room temperature. All STM images were obtained in the constant-current mode by recording the vertical tip movement.

Results

Figs. 1 and 2 show STM images of less than half a monolayer (ML) of CD deposited on Pt(111). In contrast to earlier findings on Cu(111),[12,13] the individual molecules are randomly distributed on the surface. This was observed on all samples investigated, independent of the coverage, indicating a low mobility of the molecules, which prevents the formation of molecular assemblies both on terraces and at step edges. From the appearance of the individual molecules, described below,

---

† Electronic supplementary information (ESI) available: Video of the process shown in Fig. 2. See http://www.rsc.org/suppdata/cp/b4/b406668e/

DOI: 10.1039/b406668e

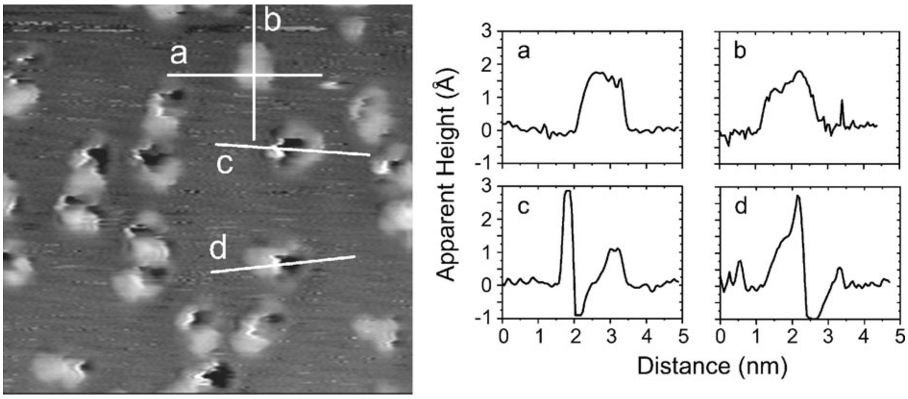

Fig. 1 STM image of cinchonidine (CD) on Pt(111). The image corresponds to the area marked in Fig. 2a. Image size: 12.5 × 12 nm, $I = 50$ pA, $U = 1.0$ V. The profiles a to d correspond to the line cuts shown in the image. (Note that, typical for STM, the molecular dimensions are somewhat bigger than anticipated from the molecular structure. Not only the local density of states of the substrate and the molecular adsorbate influence the size of the imaged surface species, but also tip convolution effects, for mere geometric reasons, generally increase their size.)

two distinct forms can be identified. Some examples are highlighted by red and green circles in Fig. 2 and hence are denominated red and green species in the following. The numerical distribution of these species did not vary in the low coverage regime investigated between 0.1 and 0.5 ml. The image sequence presented in Fig. 2 (and presented as a movie in the electronic supplementary information (ESI)†) has been taken at a rate of 52 s per image.

The appearance of the red species is characterized by three lobes forming sort of a triangular arrangement (Fig. 2). The apparent height of these molecules is around 1.5–2 Å on the full width (1.5 nm) and length (2 nm) of the molecules (see Fig. 1a and 1b). The green species have a more random shape distribution, but are identified by a characteristic apparent height profile ranging from −1 to 3 Å (Fig. 1c and d). This characteristic profile shows that the tip moves both further away from the surface and very close to the surface for each scan line contributing to the image of these molecules.

Based on this observation and the arguments below, we tentatively assign the green species as CD molecules adsorbed *via* the quinoline rings in the so called flat adsorption mode (see Fig. 3a). In such an adsorption mode the molecule is anchored strongly to the surface *via* the quinoline π-system, while the quinuclidine part points away from the surface. Therefore, the rotation of the quinuclidine moiety around the C8–C9 and the C9–C4 bonds of the molecule (see Fig. 3a) is not blocked by any interaction with the metal surface, and the molecule can adopt different conformations (*e.g.* closed(1), closed(2), open(3), closed(4) *etc.*).[17,18] This identification can explain the observed apparent height profiles in Fig. 1c and 1d: Each

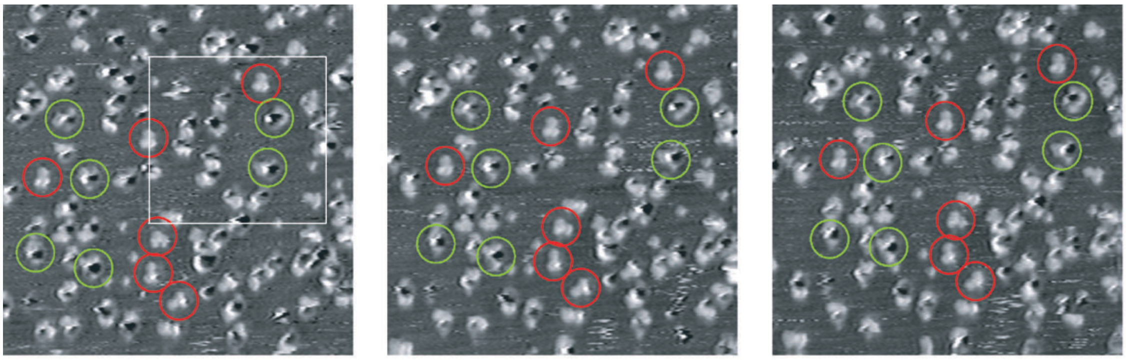

(a) 2 E-10 mbar (b) 5 E-9 mbar H2 (c) 6 E-8 mbar H2

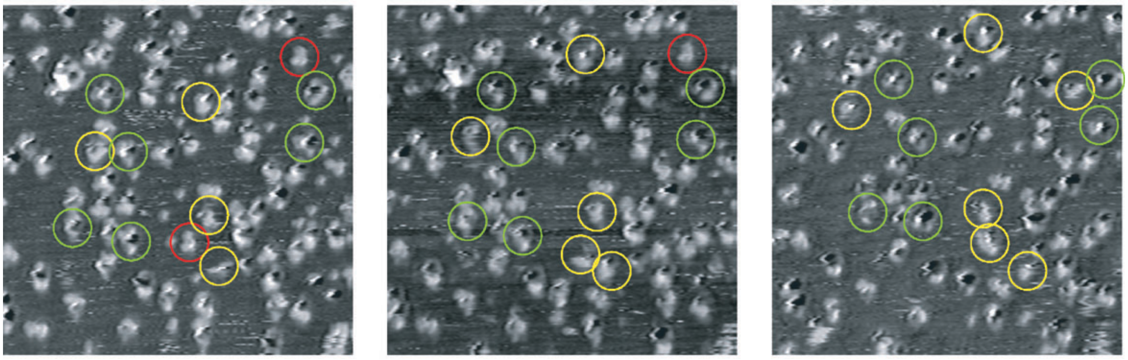

(d) 5 E-7 mbar H2 (e) 3 E-6 mbar H2 (f) 5 E-9 mbar H2

Fig. 2 STM sequence showing the evolution of the molecular adsorbates while increasing the hydrogen pressure in the chamber from 2×10^{-10} to 3×10^{-6} mbar. The selected molecules marked in red, green and yellow represent different adsorption modes of CD on Pt(111). The red species flips to a different adsorption mode (yellow) at elevated hydrogen pressure. The images selected correspond to the images number 2, 8, 12, 17, 22 and 36 of a sequence of 40 images in total. The full sequence is available as film in the supporting information. The area marked in white corresponds to the area shown in Fig. 1. Image size: 25 × 25 nm, $I = 50$ pA, $U = 1.0$ V.

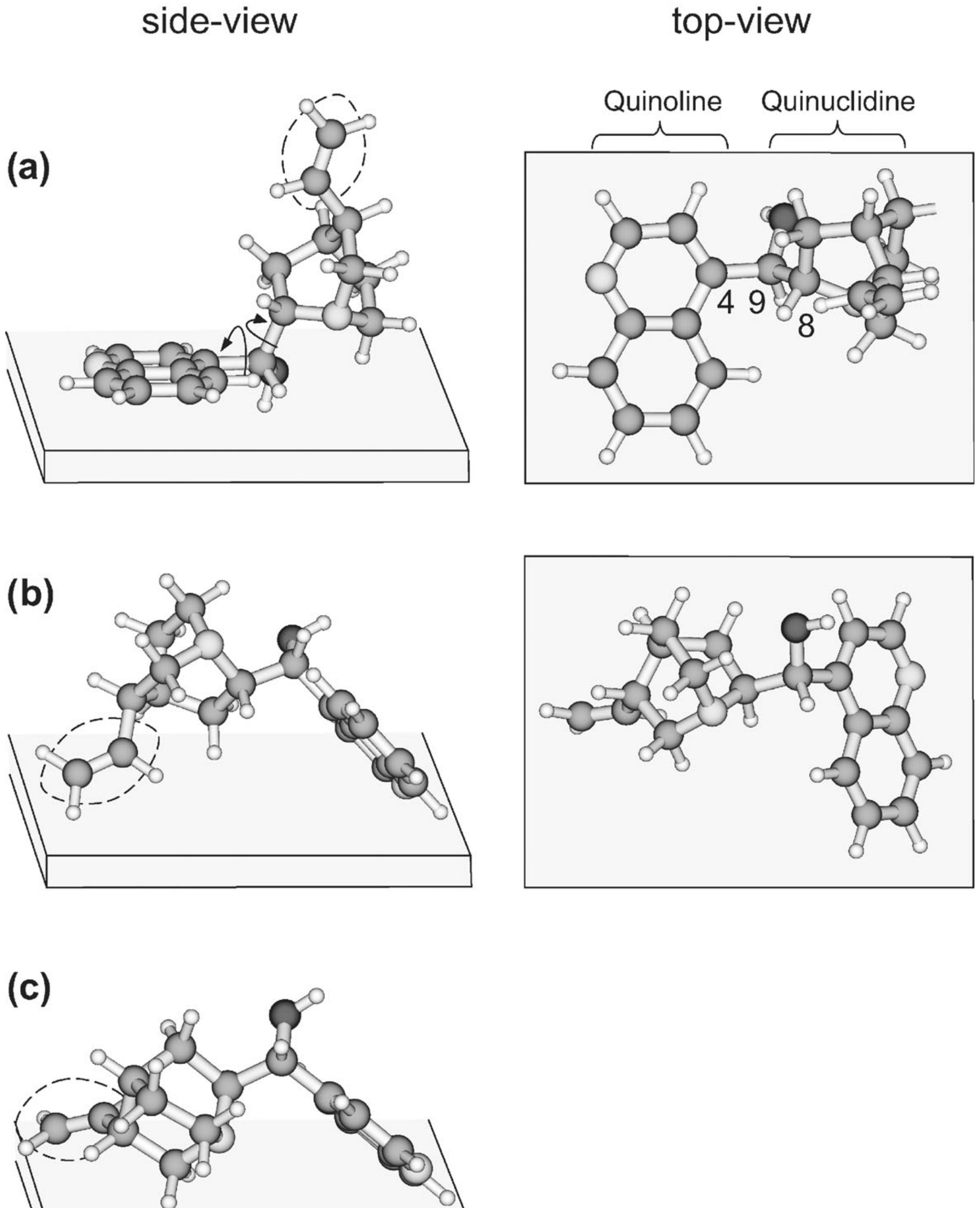

Fig. 3 Schematic top- and sideview of CD on a Pt surface. The CD structures are optimized open(3) (a and b) and closed(1) (c) structures, respectively. Molecules with the given conformation are drawn in proximity to a schematic metal surface. (a) represents the flat adsorption mode of CD (green species) while (b) and (c) represent two variations of the tilted upside-down adsorption mode (red species). The terminal $C{=}C$-double bond is marked by a dashed line.

time the STM tip approaches a flatly adsorbed CD molecule it starts to interact with the molecule and withdraws in order to maintain a constant current. The CD molecule is affected by the force induced by the tip and as a result changes its conformation. This process occurs on a timescale much faster than the feedback loop settings, which control the tip movement. As a consequence, the tip exhibits the pronounced sharp directional change shown in Fig. 1c and 1d. If the speed of the feedback is increased (decreased), the effect persists, while the characteristic profile is slightly rounded (sharpened). In other words, the appearance of the flatly adsorbed, green species as imaged by STM is partly the result of the feedback system responding to the fast change in conformation of the molecule. Due to this conformational flexibility the shape of the molecules is intrinsically not very well defined, nonetheless their appearance is very distinct (Figs. 1 and 2).

The absence of such an effect in the imaging of the red species not only leads to a more uniform appearance of the molecules, but implies that no such conformational switching takes place. As a consequence this CD species must interact differently with the metal surface and adopt another adsorption geometry compared to the green species described before.

More insight into the possible adsorption geometry of the red species was gained by the time-resolved observation of the CD molecules during a stepwise increase of the hydrogen pressure in the chamber (Figs. 2a–f and 4).

In the first period (images a–c), all molecules are virtually immobile and stay at their place up to a hydrogen pressure of 6×10^{-8} mbar. Upon a further increase in hydrogen pressure, four out of six molecules of the red species change their appearance (image c to d). These molecules are marked yellow. Similar to our observations with the green species (tentatively assigned as flatly adsorbed molecules), the appearance of these molecules marked in yellow is dominated by a characteristic, sharp profile. Therefore, we suggest that these CD molecules have changed the adsorption mode in a way which releases the quinuclidine part of the molecule from a fixed to a free position. It is important to note that this transformation was induced by the presence of hydrogen on the Pt surface. When no hydrogen was available in the chamber, we never observed such a transformation. Furthermore the transformation was irreversible. After closing the leak valve, no back-conversion from the yellow to the red species was observed, as illustrated in image f. Note also that a few smaller adsorbates (*e.g.* in the lower left quadrant of the image series), not discussed so far, are desorbing from the surface at elevated hydrogen pressure. We consider these adsorbates being impurities brought onto the surface during the evaporation of CD. Obviously, the presence of hydrogen leads to the removal of small surface impurities, in analogy to the cleaning effect observed during *in situ* ATR-IR investigations on Pt.[19] The full image sequence consisting of 40 images is available as ESI.† The changes in adsorption geometry and the surface dynamics of the different species can be seen best in this movie, as the static representation by six snapshots in Fig. 2 can not illustrate the entire information.

On the basis of these experiments, we tentatively assign the red species to a tilted upside-down adsorption mode, similar to the one shown in Fig. 3b. In this illustration the open(3) conformer, which is the most stable in gas phase,[17] is placed in an upside-down fashion on the schematic Pt surface. Compared to a flat adsorption (Fig. 3a) the adsorption energy is expected to be lower because the interaction between the aromatic moiety and the Pt surface is weakened, if they are not parallel.[20] However, some adsorption energy is gained by the additional interaction of the terminal $C{=}C$ double bond and the quinuclidine N atom (Fig. 3b and c), which are brought into close proximity with the Pt surface. Through this additional interaction the position of the quinuclidine moiety is fixed, explaining the lack of the sharp dark-bright feature in the images of this species. With increasing hydrogen pressure the terminal $C{=}C$-double bond can undergo hydrogenation,[15,16] which weakens the bonding of this part of the molecule to the surface. Hence the molecule flips to an energetically more favourable adsorption mode similar to the flat adsorption mode shown in Fig. 3a.

Despite the similarities between the yellow species and the flatly adsorbed molecules, there is a significant difference between them concerning the surface mobility. It can be seen in Fig. 2d–f (and in the movie) that the yellow species change positions within the image sequence. They have a higher mobility than both the flatly adsorbed as well as the tilted upside-down molecules. The change in mobility concomitant with the flipping of the adsorption mode is shown in Fig. 4, where the integral displacement d for each of the six molecules marked in red (later yellow) and green is shown. Note that, in addition to the appearance of the molecules in the STM images, the different surface mobilities of the adsorbed species is an additional, very strong argument for the discrimination of different surface species. This increased mobility is further confirmed by these molecule's appearance in STM: they move slightly under the influence of the tip during the imaging process, which leads to a "jagged" outline. This makes it more difficult to identify a precise adsorption mode of this yellow species. However, we suggest an adsorption mode similar to the flat one depicted in Fig. 3a. The higher mobility may be due to a partial hydrogenation of the aromatic ring system. This partial hydrogenation is known to occur as a side reaction during the catalytic process, weakening the adsorption strength of CD, and decreasing the efficiency of this catalyst system.[21,22] Interestingly, only those molecules which have been converted from the red into the yellow species exhibit an increased mobility in our experiments. We may thus speculate, that during this transformation, the molecules have a higher activity towards hydrogenation than the green species which we observe to be inert in our experimental sequence.

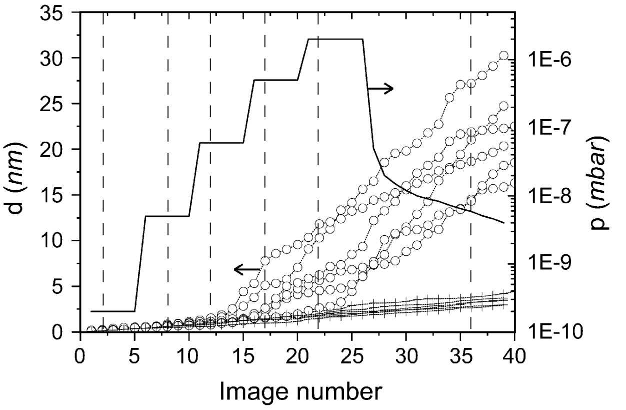

Fig. 4 Effect of the hydrogen pressure p on the mobility of the green (crosses) and the red (circles) species during the full sequence of 40 images taken. The integral displacement d of the molecules is displayed *versus* the image number. The mobility is initiated by the hydrogen-induced transformation of the red into the yellow species and persists when the hydrogen pressure is lowered again. The dashed lines mark the images displayed in Fig. 2a–f.

Discussion

For the sake of clarity not all molecules in Figs. 1 and 2 have been marked as green, red or yellow species. However, it can be seen easily, that the majority of those molecules which have not been marked, are characterized by the sharp dark-bright feature typical for the green species. If all molecules are summed over, almost 90% of the CD molecules adopt this flat adsorption mode. This interpretation is supported by the fact that all these molecules are virtually immobile, very much the same as the six selected molecules which have been marked with a green circle.

Unfortunately, there is no direct proof for the adsorption geometries we suggest in Fig. 3. However we could not identify any other adsorption geometry of CD which could explain both the very low mobility of the molecules on Pt(111) and the flexibility of the quinuclidine moiety we observed for the green species. Furthermore, recent calculations showed that such an adsorption geometry of CD is very stable on Pt(111).[20] Still, with the resolution, which is possible to obtain in room temperature STM, we cannot exclude that the full population of the green species consists of different adsorption geometries which differ from the one shown in Fig. 3a in some respect as *e.g.* (i) the precise angle between the Pt surface and the plane of the quinoline ring or (ii) the rotation of the quinoline ring around the C4–C9 bond by 180°, discriminating between open(3) and open(4) or closed(1) and closed(2) conformations.

For the adsorption geometry of the red species the situation is less evident. Besides the adsorption geometry shown in Fig. 3b and 3c, other structures, where the quinuclidine part of CD is fixed to the surface by an additional interaction are possible. Such a structure bearing the potential for the hydrogenation of the terminal C=C double bond has been found recently through calculations.[20]

It is interesting to compare our STM data with the wealth of spectroscopic and catalytic data available for the Pt/CD system. Even though the results presented here have been measured at conditions far from the real catalysis conditions (pressure gap) there is a good level of agreement with the findings obtained by other techniques. For example, the predominantly flat adsorption as well as the existence of tilted (mainly at higher coverage) adsorption modes has been observed by different spectroscopic methods.[15,16,23] The importance of flat adsorption of CD has also been demonstrated by catalytic studies.[24] The hydrogenation of the terminal C=C-double bond is known to occur fast under catalytic conditions and during *in situ* ATR-IR spectroscopy,[15,16,21] and the partial hydrogenation of the aromatic moiety of CD and its consequences for enantioselective hydrogenation have been investigated by various groups.[21,22,25] Finally, the very low surface mobility observed for most CD species is also in agreement with the observation of Bakos *et al.*, who showed by cyclic voltametry that the adsorption of CD on Pt is irreversible.[26]

The random distribution of the CD molecules on the whole Pt(111) surface, independent of coverage, stands in contrast to findings recently reported on copper.[12,13] Due to the much stronger interaction of the molecules with Pt the formation of an ordered assembly is not possible. Future investigations should therefore focus on Pt, as the investigation of CD on nonreactive metals such as Cu are likely to be of no or minor relevance concerning the surface processes involved in asymmetric catalysis.

Compared to all other catalytic and spectroscopic techniques, the fundamental difference of our STM approach lies in the fact that we can gain information on the level of single molecules and follow their behaviour with time. This is particularly advantageous because in heterogeneous catalytic processes it is impossible to know *a priori* whether the most abundant surface species is also the most relevant for the catalytic process. The discrimination of different surface species by their mobility and the time-resolved observation of their surface chemical processes provides a powerful tool for the investigation of complex catalyst systems such as the Pt/CD system.

The results presented in this paper clearly demonstrate the feasibility of such an approach. The ultimate goal will be the elucidation of the surface processes involved in the enantiodiscrimination on a single molecule level.

Acknowledgements

We thank Prof. H.-J. Güntherodt for his support of the Nanolab. We thank Nanonis Inc. for the fruitful collaboration on the data aquisition and the control unit. The technical support by A. Heuri is gratefully acknowledged. Financial support from the Swiss National Science Foundation is kindly acknowledged. T. A. Jung and M. von Arx acknowledge the support by the NCCR on Nanoscale Science.

References

1 F. Schreiber, *Prog. Surf. Sci.*, 2000, **65**, 151.

2 J. V. Barth, J. Weckesser, G. Trimarchi, M. Vladimirova, A. De Vita, C. Cai, H. Brune, P. Gunter and K. Kern, *J. Am. Chem. Soc.*, 2002, **124**, 7991.

3 M. De Wild, S. Berner, H. Suzuki, H. Yanagi, D. Schlettwein, A. Baratoff, H.-J. Güntherodt and T. A. Jung, *ChemPhysChem*, 2002, **3**, 881.

4 (*a*) T. Osawa, T. Harada and O. Takayasu, *Top. Catal.*, 2000, **13**, 155; (*b*) T. Sugimura, *Catal. Surv. Jpn.*, 1999, **3**, 37.

5 (*a*) M. von Arx, T. Mallat and A. Baiker, *Top. Catal.*, 2002, **19**, 75; (*b*) M. Studer, H. U. Blaser and C. Exner, *Adv. Synth. Catal.*, 2003, **345**, 45; (*c*) P. B. Wells and A. G. Wilkinson, *Top. Catal.*, 1998, **5**, 39.

6 (*a*) W. R. Huck, T. Mallat and A. Baiker, *New J. Chem.*, 2002, **26**, 6; (*b*) A. Tungler, T. Tarnai, L. Hegedüs, K. Fodor and T. Mathe, *Platinum Met. Rev.*, 1998, **42**, 108; (*c*) Y. Nitta and A. Shibata, *Chem. Lett.*, 1998, **2**, 161.

7 M. O. Lorenzo, C. J. Baddeley, C. Muryn and R. Raval, *Nature*, 2000, **404**, 376.

8 (*a*) V. Humblot, S. Haq, C. Muryn, W. A. Hofer and R. Raval, *J. Am. Chem. Soc.*, 2002, **124**, 503; (*b*) T. E. Jones and C. J. Baddeley, *Surf. Sci.*, 2002, **513**, 453.

9 J. M. Bonello, R. M. Lambert, N. Künzle and A. Baiker, *J. Am. Chem. Soc.*, 2000, **122**, 9864.

10 J. M. Bonello, F. J. Williams and R. M. Lambert, *J. Am. Chem. Soc.*, 2003, **125**, 2723.

11 T. Heinz, G. Wang, A. Pfaltz, B. Minder, M. Schürch, T. Mallat and A. Baiker, *Chem. Commun.*, 1995, 1421.

12 Q.-M. Xu, D. Wang, L.-J. Wan, C.-L. Bai and Y. Wang, *J. Am. Chem. Soc.*, 2002, **124**, 14300.

13 Q.-M. Xu, D. Wang, M.-J. Han, L.-J. Wan and C.-L. Bai, *Langmuir*, 2004, **20**, 3006.

14 T. Evans, A. P. Woodhead, A. Gutierrez-Sosa, G. Thornton, T. J. Hall, A. A. Davis, N. A. Young, P. B. Wells, R. J. Oldman, O. Plashkevych, O. Vahtras, H. Agren and V. Carravetta, *Surf. Sci.*, 1999, L691.

15 D. Ferri, T. Bürgi and A. Baiker, *Chem. Commun.*, 2001, 1172.

16 D. Ferri and T. Bürgi, *J. Am. Chem. Soc.*, 2001, **123**, 12074.

17 T. Bürgi and A. Baiker, *J. Am. Chem. Soc.*, 1998, **120**, 12920.

18 G. D. H. Dijkstra, R. M. Kellog, H. Wynberg, J. S. Svendson, I. Marko and K. B. Sharpless, *J. Am. Chem. Soc.*, 1989, **111**, 8069.

19 D. Ferri, T. Bürgi and A. Baiker, *J. Phys. Chem. B*, 2001, **105**, 3187.

20 (*a*) A. Vargas, T. Bürgi and A. Baiker, *J. Catal.*, 2004, **226**, 69; (*b*) S. R. Calvo, R. J. LeBlanc, C. T. Williams and P. B. Balbuena, *Surf. Sci.*, 2004, **563**, 57.

21 H. U. Blaser, H. P. Jalett, W. Lottenbach and M. Studer, *J. Am. Chem. Soc.*, 2000, **122**, 12675.

22 M. Bartok, T. Bartok, G. Szöllösi and K. Felföldi, *Catal. Lett.*, 1999, **61**, 57.

23 J. M. Bonello, R. Lindsay, A. K. Santra and R. M. Lambert, *J. Phys. Chem. B*, 2002, **106**, 2672.

24 S. Diezi, A. Szabo, T. Mallat and A. Baiker, *Tetrahedron Asymmetry*, 2003, **14**, 257.

25 W. R. Huck, T. Bürgi, T. Mallat and A. Baiker, *J. Catal.*, 2003, **216**, 276.

26 I. Bakos, S. Szabo, M. Bartok and E. Kalaman, *J. Electroanal. Chem.*, 2002, **532**, 113.